

Photocatalysis by Calcium Hydroxyapatite Modified with Ti (IV)

● Masato Wakamura

(Manuscript received February 3, 2005)

Colloidal $\text{Ca}_{10}(\text{PO}_4)_6(\text{OH})_2$ hydroxyapatite (HAP) particles doped with Ti(IV) ions in different atomic ratios, $\text{Ti} / (\text{Ca} + \text{Ti}) = X_{\text{Ti}}$, by a coprecipitation method were characterized by JEOL transmission electron microscope (TEM), UV, Elmer Fourier transform infrared (FTIR) spectrophotometer, X-ray photoelectron spectroscopy (XPS), and Perkin-Elmer-induced coupled plasma spectrometer (ICP-AES). The photocatalytic activity of the modified HAP particles was examined by decomposition of acetaldehyde and albumin and bactericidal test by colon bacilli. The deodorization ability was measured using a six-stage sensory method. Ca(II) of HAP was substituted by Ti(IV) in a one-to-one ratio at $X_{\text{Ti}} \leq 0.1$. When doped at $X_{\text{Ti}} > 0.1$, irregular particles of amorphous titanium phosphate were formed besides long, rectangular particles of HAP. X_{Ti} of the surface phase of the particles was much less than that of the whole particles; Ti(IV) is less contained in the surface phase than the bulk one. A UV beam was absorbed by Ti(IV)-modified HAP particles but not by the unmodified particles. The decomposition of acetaldehyde and albumin by Ti(IV)-doped particles was found under UV irradiation, while the unmodified HAP particles were inactive for the decomposition of both materials. Further, unlike TiO_2 , Ti(IV)-doped HAP showed a bactericidal function in the dark. A Ti(IV)-doped HAP adhesion filter demonstrates a high deodorization performance.

1. Introduction

Recently, titanium dioxide, TiO_2 , has been receiving much attention as a photocatalyst that photo-oxidizes organic substances in both water and air.^{1,2)} Synthetic calcium hydroxyapatite $\text{Ca}_{10}(\text{PO}_4)_6(\text{OH})_2$, referred to as hydroxyapatite (HAP), is biologically important and is used as a bioceramic and adsorbent for biomaterials because it shows an excellent affinity for organic compounds such as proteins. Hence, it is of interest for preparing composite materials of TiO_2 and HAP for photocatalytic decomposition of biomaterials such as proteins and lipids. Nonami et al. proposed a new structure for TiO_2 -HAP composite films in which a porous HAP layer forms on a TiO_2 layer on a substrate in a pseudo body solution.³⁾ However, this composite structure is

inefficient for photocatalysis, which requires UV irradiation of the TiO_2 layer. We attempted to develop a novel photocatalyst with a high affinity for biomaterials by atomic-level composition of a photocatalytic material and HAP, which was realized by modifying HAP particles with Ti(IV). The modification of HAP particles was performed by coprecipitation and ion exchange methods. Suzuki et al. have found that Ca(II) of HAP can be exchanged with various metal ions in aqueous media.⁴⁻¹²⁾ However, the surface structure and properties of the metal-substituted HAP have not been clarified. Ribeiro et al. have studied the surface of HAP modified with Ti(IV) ions by immersion methods¹³⁾ and indicated the formation of a titanium phosphate, $\text{Ti}(\text{HPO}_4)_2 \cdot n\text{H}_2\text{O}$ ($n = 1-3$), which probably has a double-layered

structure.¹⁴⁾ Weiser et al. have coated metal Ti with HAP by doping and diffusing Ca and P elements into the metal before the coating to obtain a high-quality HAP film on the metal Ti surface.¹⁵⁾ On the other hand, Zeng et al. have studied the adsorption of albumin on calcium phosphate (CaP) and Ti films deposited on a germanium ATR crystal by ion beam sputter deposition from HAP and metal Ti targets and found that the CaP film adsorbs greater amounts of albumin than the surface of metal Ti; CaP shows a higher affinity for protein than metal Ti.¹⁶⁾ Since the HAP surface is known to show a high affinity for albumin,^{17),18)} HAP is used as an adsorbent in column chromatography for separating proteins. The bactericidal effects of Ag-HAP thin films on alumina have been reported by Feng et al.¹⁹⁾ Although Ti(IV)-modified HAP is anticipated to show a bactericidal effect, there has been no study on the bactericidal characteristics of this material.

Wakamura et al. previously investigated the surface structure and composition of HAP particles modified with various metal ions by coprecipitation and ion-exchange methods.²⁰⁾⁻²²⁾ In the present study, HAP particles modified with Ti(IV) by a coprecipitation method were characterized by various techniques. The photocatalytic activities of the well-characterized modified HAP particles were examined by decomposition reactions of acetaldehyde and albumin.

The deodorization ability of an adhesion filter incorporating the modified HAP particles was evaluated using a sensory six-stage odor-strength method.

Based on the obtained results, we examined the surface structure and photocatalysis of the modified HAP particles. Further, the bactericidal function of the materials was examined using a colon bacillus²³⁾ and a noble photocatalyst was developed.

2. Experiments

2.1 Materials

Colloidal HAP particles doped with Ti(IV)

were prepared by coprecipitation; $\text{Ca}(\text{NO}_3)_2$ and $\text{Ti}(\text{SO}_4)_2$ were dissolved in 1 dm³ deionized-distilled water free from CO₂ at different atomic ratios: $\text{Ti} / (\text{Ca} + \text{Ti}) = X_{\text{Ti}}$ from 0 to 0.8. The total amount of Ca and Ti in the solutions was held at 0.1 mol; 0.060 mol H₃PO₄ was added to the solutions, and the solution pH was adjusted to 9 by adding a 15 mol dm⁻³ NH₄OH solution. The resulting suspension was aged in a capped Teflon vessel at 100°C for 6 h. The resulting precipitates were filtered off, washed with 5 dm³ deionized and distilled water, and finally dried in an air oven at 70°C. Ninhydrin and albumin supplied by Wako Pure Chemicals were used as received.

2.2 Characterization

The HAP particles thus modified with Ti(IV) were examined by various conventional methods as follows. The morphology of the particles was observed using a JEOL transmission electron microscope (TEM) at an accelerating voltage of 200 kV. The samples for TEM were prepared by a dispersing method. X-ray diffraction (XRD) patterns were taken by a powder method using a Shimadzu high-intensity diffractometer with a rotating cathode using CuK α radiation (50 kV and 200 mA). Transmission IR spectra were recorded in vacuo using a Perkin-Elmer Fourier transform infrared (FTIR) spectrophotometer using a self-supporting disk method in a vacuum cell. The sample powders (30 mg) were pressed into disks of 1 cm diameter under 572 kg cm⁻². Before taking the spectra, the sample disks were outgassed at 300°C for 2 h. Reflection UV-VIS spectra were taken using a UV spectrometer (JASCO V-560) at 200 to 400 nm. The specific surface area was calculated by applying the BET equation to the N₂ adsorption isotherm measured at -196°C using an automatic volumetric apparatus.

2.3 Chemical analysis

The Ti and P contents were determined by a Perkin-Elmer-induced coupled plasma spectrometer (ICP-AES) employing wavelengths of 317.933

(Ca), 334.941 (Ti), and 213.618 nm (P). The samples for ICP-AES were dissolved in a dilute HNO₃ solution. X-ray photoelectron spectroscopy (XPS) was done using a Perkin-Elmer spectrophotometer with MgK α radiation (20 kV and 30 mA), with the samples mounted on the sample holder by carbon tape.

2.4 Acetaldehyde decomposition test

The photocatalytic activities were estimated from decomposition of acetaldehyde vapor under 1 mW cm⁻² UV irradiation. The samples used for photocatalysis were HAP modified at X_{Ti} = 0 and 0.1. The sample weight was decided by adjusting the surface area of the samples to a constant value of 85 m² using the BET-calculated surface area. The samples were settled in the bottom of a 500 cm³ cylindrical glass vessel sealed using a 5 mm-thick quartz plate with an O-ring. The air was replaced by a mixed gas (N₂: 80%, O₂: 20%) introduced into the vessel through the gas inlet, and then acetaldehyde vapor was injected into the vessel and the vessel was stored in darkness to achieve equilibrium. Then, irradiation by ultraviolet light at 1 mW cm⁻² followed by further storage in darkness were repeated at 24 h intervals. After the reaction, the concentrations of acetaldehyde and CO₂ in the reaction vessel were determined using a gas chromatograph (FID).

2.5 Ninhydrin test of albumin decomposition.

The affinity for biomaterials and photocatalytic activities were estimated from adsorption and decomposition of albumin. The ninhydrin test was employed to identify albumin before and after the decomposition reaction. Samples of 1 g HAP modified at X_{Ti} = 0 and 0.1 and 1 g TiO₂ were immersed in 1 g dm⁻³ albumin solutions at 30°C for 12 h. The particles were filtered, washed with 10 dm³ deionized distilled water, and dried in an air oven at 50°C. Each sample was divided into two 0.5 g parts; one was kept in a lightproof box and another

was irradiated by 1 mW cm⁻² UV light for 24 h at room temperature. Finally, the samples were sprayed with a ninhydrin indicator and dried in an air oven at 150°C.

2.6 Bactericidal test by *Escherichia coli* (*E. coli*)

The suspensions of HAP modified at X_{Ti} = 0 and 0.1 and TiO₂ homogeneously dispersed in silica sols were deposited on glass plates (5 × 5 cm) by a spin-coating method. The films on glass were sterilized by drying at 180°C for 30 min. *E. coli* cells (IFO 3310 strain) were grown aerobically in 2.5 cm³ of nutrient broth (Daigo: Nippon Seiyaku) at 30°C for 16 to 18 h. The cells were centrifuged at 4000 rev min⁻¹ and suspended in sterilized water with appropriate dilution. *E. coli* cell suspensions (150 × 10⁻⁶ dm³, 2 × 10⁵ cells cm⁻³, total 3 × 10⁴ cells) were pipetted onto glass plates coated with HAPs (modified at X_{Ti} = 0 and 0.1) and TiO₂, spread out to form a liquid film of approximately 1 cm in diameter, and placed in an airtight illumination chamber to prevent drying. The chamber was illuminated with a 15 W black light, and the light intensity as measured using a UV radiometer (UVR-36, Tepcon) at the sample position was 1.0 mW cm⁻² with peaks at around 360 nm. After the illumination, the cells were removed using a gauze patch and collected in a 0.15 mol dm⁻³ NaCl solution. This solution was spread onto nutrient agar medium (Nissui: Standard Method Agar, Nissui Seiyaku) and incubated for 24 h to determine the number of viable cells in terms of colony-forming units.

2.7 Deodorization ability test

We made an air cleaner that uses an adhesion filter incorporating HAP modified at X_{Ti} = 0.1.

The air cleaner was placed in a 1 m³ box filled with the odors of cigarettes and rotten fish, and the strength change in these odors was assessed using a six-stage sensory method.

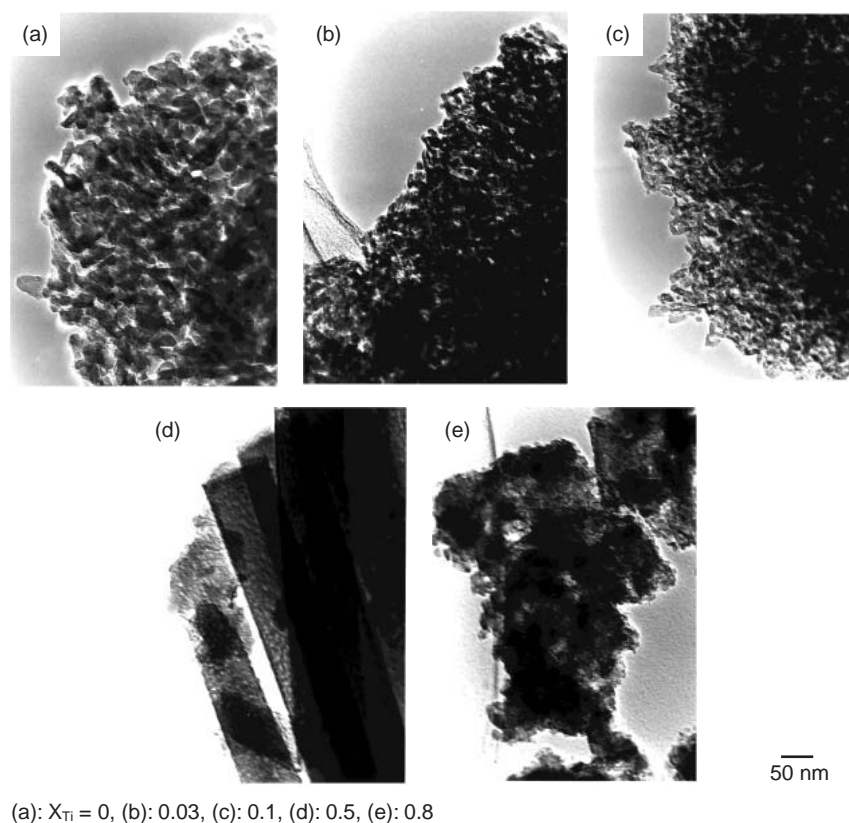


Figure 1
TEM micrographs of particles formed at various X_{Ti} by coprecipitation.

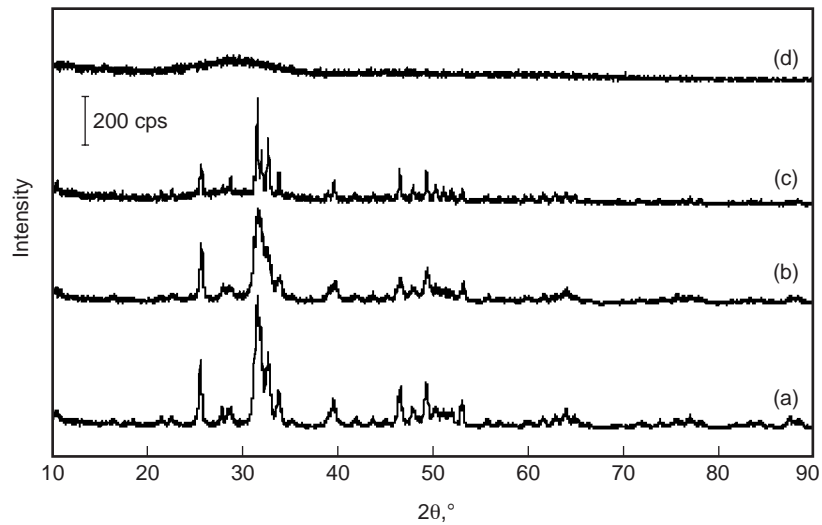
3. Results and discussion

Figure 1 shows TEM micrographs of Ti(IV)-doped HAP particles. The HAP particles formed at $X_{Ti} \leq 0.1$ are short rods. The particles formed at $X_{Ti} \geq 0.5$ are a mixture of long rectangular and irregular particles, although Figures 1 (d) and (e) show only long rectangular and irregular particles, respectively. The irregular particles increased with an increase of X_{Ti} . Although the detailed reason for the formation of the long particles remains unclear, the charge difference between Ca(II) and Ti(IV) seems to influence the particle formation of HAP, as was found in a previous study on modification with Cr(III).¹⁹⁾

Figure 2 shows XRD patterns of the products at different X_{Ti} . Their peak intensity was lowered by increasing X_{Ti} at $X_{Ti} \leq 0.5$, and the products at $X_{Ti} = 0.8$ were poorly crystallized. Except for the product at $X_{Ti} = 0.8$, the patterns

are characteristic of HAP (JPCDS 9-432), verifying that the long rectangular particles formed at $X_{Ti} \geq 0.5$ are well-crystallized HAP. This finding suggests that HAP crystals can be doped with Ti(IV) up to $X_{Ti} = 0.1$.

To determine the composition of the products, Ca, Ti, and P in the formed particles were assayed by ICP-AES. **Figure 3** plots the Ca(II) and Ti(IV) ion contents against X_{Ti} with triangles and circles, respectively. The increase of Ti(IV) in the formed particles accompanies an equivalent decrease of Ca(II), which means that Ti(IV) in the crystal of HAP is present as a divalent ion such as $[Ti(OH)_2]^{2+}$ or $[Ti(HPO_4)]^{2+}$. **Figure 4** plots X_{Ti} of whole particles and the surface phase of particles as determined by ICP-AES and XPS, respectively. For all the materials, X_{Ti} of the surface phase (X_s) was less than that of whole particles (X_w), which can be interpreted by considering that



(a): $X_{Ti} = 0$, (b): 0.1, (c): 0.5, (d): 0.8

Figure 2
XRD patterns of products at various X_{Ti} by coprecipitation.

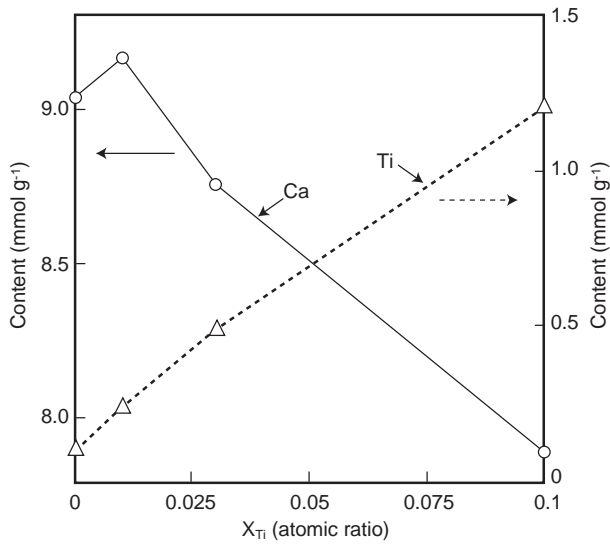
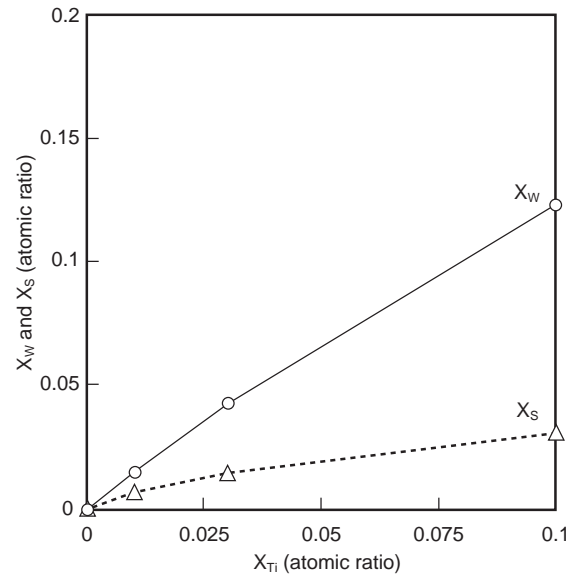


Figure 3
Ca and Ti contents vs. X_{Ti} .



X_w : ratio in whole particles, X_s : ratio in surface phase.

Figure 4
Atomic ratios X_{Ti} of Ti(IV)-modified HAP particles.

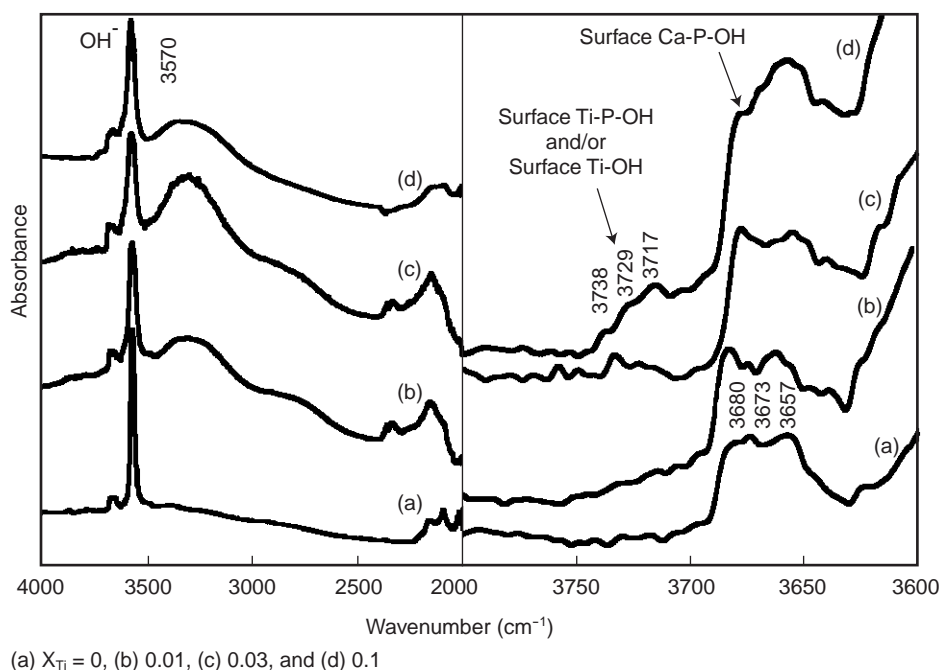


Figure 5
IR spectra of HAP particles modified with Ti(IV) by coprecipitation at various X_{Ti} .

Ti(IV) is precipitated more easily than Ca(II) and therefore X_{Ti} will be higher in the inner part of particles. X_w is larger than X_{Ti} in the starting solutions, implying that Ti(IV) is incorporated into the particles more than Ca(II). These results are ascribed to the fact that Ti(IV) has a higher hydrolysis constant than Ca(II).

Figure 5 shows FTIR spectra of the HAP particles modified with Ti(IV). The spectrum of the sample formed at $X_{Ti} = 0$ gives rise to three bands at 3680, 3673, and 3657 cm^{-1} (a). We previously assigned these three bands to the O-H stretching vibration modes of surface P-OH groups, which are considered to form due to protonation of surface PO_4^{3-} ions to balance the surface charge.²⁴⁾ The spectrum of the samples formed at $X_{Ti} = 0.1$ shows three additional IR bands at 3738, 3729, and 3717 cm^{-1} that would be ascribed to surface Ti-OH groups (c).

Figure 6 shows the reflection UV-VIS spectra of the products at varied X_{Ti} along with the spectrum of TiO_2 [(d)]. The UV absorption

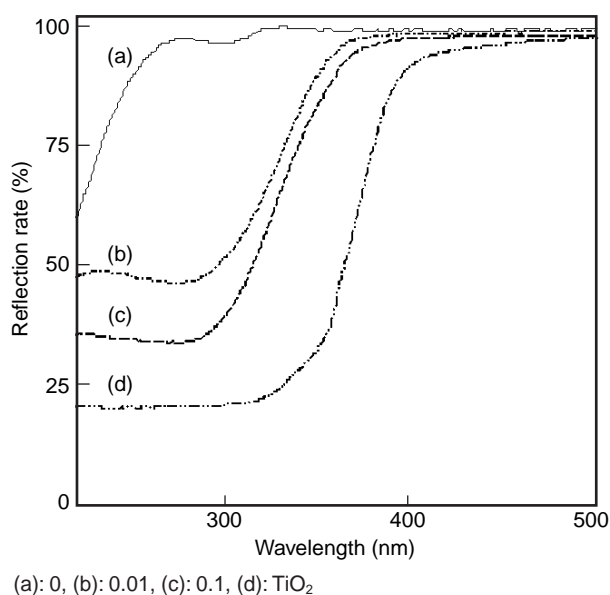


Figure 6
Reflection UV-VIS spectra of HAP particles modified with Ti(IV) by coprecipitation at various X_{Ti} and TiO_2 .

above ca. 370 nm is observed in the samples modified at $X_{Ti} = 0.01$ and 0.1 [(b) and (c)], but not in the unmodified HAP [(a)]. As X_{Ti} increases, the absorbance rises to that of TiO_2 . These results clearly imply that the surface of HAP particles is modified by substitution with Ti(IV).

Figure 7 plots the concentrations of acetaldehyde and CO_2 against the UV irradiation time. It is clearly seen in Figure 7 (b) that 1) CO_2 is increased (open circles) and acetaldehyde is decreased (closed circles) by irradiating the material modified at $X_{Ti} = 0.1$ and 2) on stopping the irradiation, the concentrations of acetaldehyde and CO_2 are essentially unchanged. Whereas, as shown in Figure 7 (a), the unmodified sample shows a smaller concentration change of CO_2 and acetaldehyde than the modified sample. Therefore, it can be confirmed that Ti(IV)-modified HAP exhibits a higher photocatalytic activity than the unmodified HAP.

Figure 8 shows the results of the ninhydrin color test: the photographs of TiO_2 [(a)], unmodified HAP [(b)], and Ti(IV)-modified HAP [(c)] irradiated and non-irradiated by UV after albumin adsorption. TiO_2 shows no ninhydrin color under UV irradiation and non-irradiation,

although a slight blue color is detected due to strongly adsorbed albumin. The unmodified HAP is colored by ninhydrin under UV irradiation and non-irradiation. The Ti(IV)-modified HAP is colored only under UV non-irradiation. These results indicate that TiO_2 does not strongly adsorb albumin, whereas the unmodified HAP adsorbs albumin but shows no photocatalytic decomposition activity and Ti(IV)-modified HAP adsorbs albumin and decomposes it by photocatalysis.

Figure 9 compares the results of the bactericidal test for the colon bacilli. TiO_2 gives rise to essentially no photocatalysis in the dark and kills only less than 10% of the bacilli, while TiO_2 kills 80% of the bacilli under UV irradiation. On the other hand, Ti(IV)-modified and unmodified HAPs show bactericidal effects even in the dark, killing ca. 50% of the bacilli. It should be noted that the bactericidal effect of Ti(IV)-modified HAP was enhanced by UV irradiation and only ca. 30% of the bacilli survived after UV irradiation. These findings indicate that Ti(IV)-modified HAP exhibits a higher bactericidal effect than TiO_2 , both in the dark and under UV irradiation.

Figure 10 shows the results of the sensory

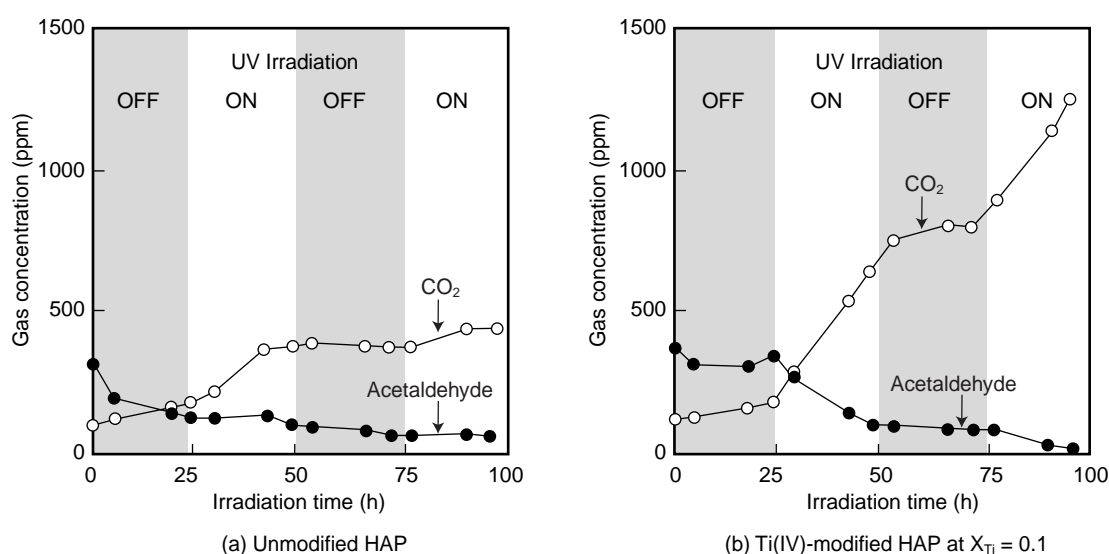


Figure 7
Concentrations of acetaldehyde (closed symbols) and CO_2 (open symbols) vs. UV irradiation time.

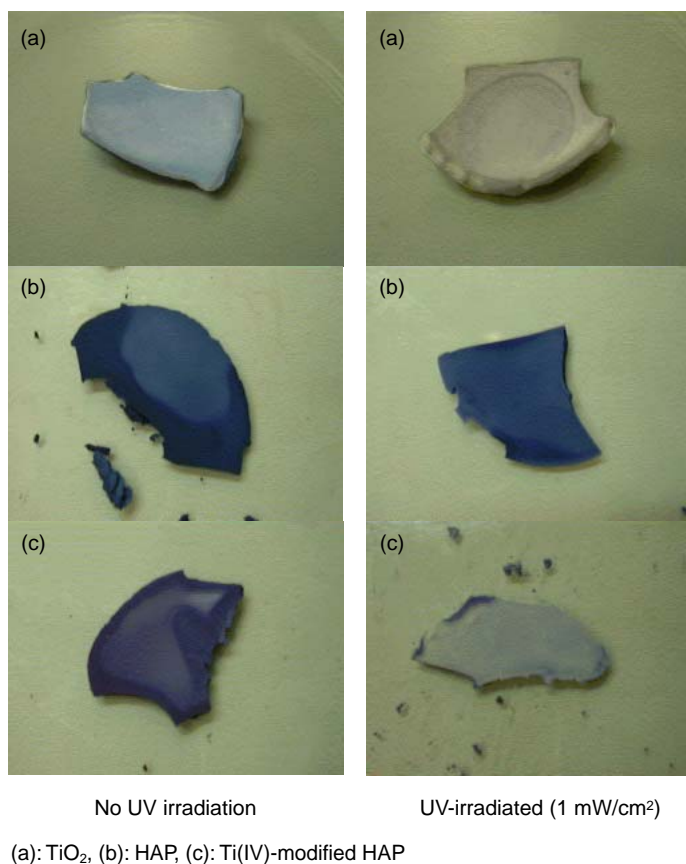


Figure 8
Results of adsorption and photocatalytic decomposition of albumin obtained by ninhydrin colored tests.

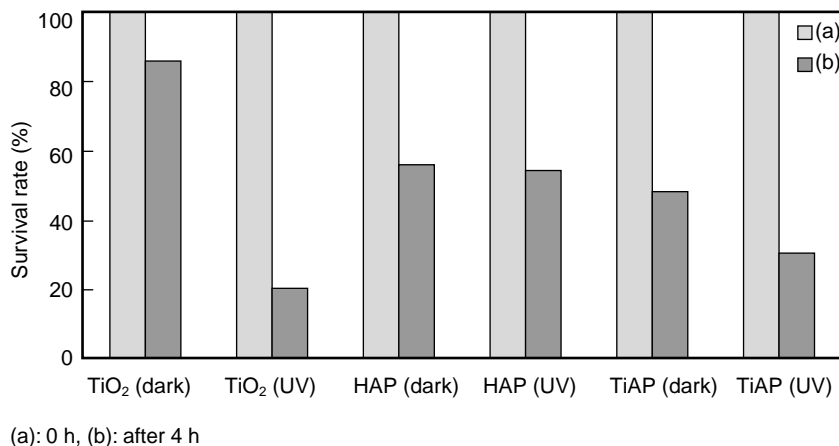


Figure 9
Results of bactericidal test using colon bacillus.

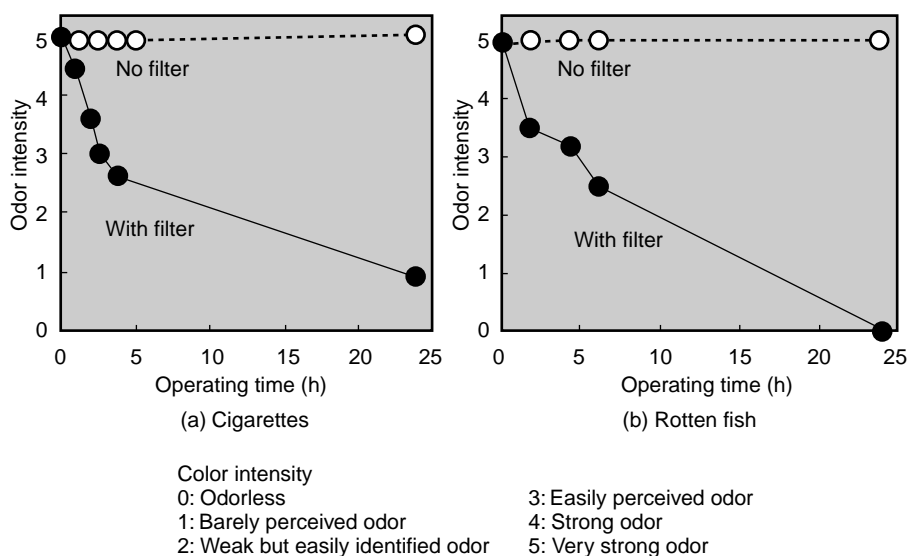


Figure 10
Results of sensory six-stage odor intensity test.

six-stage odor-strength test. As can be seen, there is a high deodorization of cigarette and rotten fish odors.

The Ti(IV)-modified HAP generates positive holes (h^+) as well as TiO_2 catalysts. These positive holes interact with adsorbed H_2O to yield hydroxyl radicals (OH^\cdot), which have a strong oxidation ability that decomposes various organic compounds and have a bactericidal effect. To verify the details of this mechanism, further analysis of the band structure of Ti(IV)-modified HAP is required.

4. Conclusion

We can draw the following conclusions from the results obtained from this study. Ca(II) ions in HAP crystals are exchanged with Ti(IV) up to atomic ratios of $X_{Ti} = 0.1$. The added Ti(IV) exists in HAP crystals as divalent cations such as $[Ti(OH)_2]^{2+}$ and $[TiHPO_4]^{2+}$. Ti(IV)-substituted HAP has surface OH groups originating from HPO_4^{2-} and OH^- coordinating to Ti(IV). HAP particles penetrated by Ti(IV) absorb UV light at wavelengths less than 380 nm, so they exhibit photocatalytic activity in the oxidation and decom-

position of acetaldehyde. This characteristic of Ti(IV)-modified HAP resembles the case of oxidative decomposition of organisms by TiO_2 . However, HAP has a high affinity for organic compounds such as proteins, although TiO_2 shows no such affinity. Therefore, distinct from TiO_2 photocatalysts, Ti(IV)-modified HAP has both an adsorption affinity and photocatalytic activity for organic compounds. To make matters better, Ti(IV)-modified HAP shows a bactericidal effect even in the dark, whereas TiO_2 shows it only under UV irradiation.

References

- 1) A. Fujishima and K. Honda: Photosensitive electrode reactions. III. Electrochemical evidence for the mechanism of the primary stage of photosynthesis. *Bull. Chem. Soc. Jpn.*, **44**, 4, p.1148-1150 (1971).
- 2) A. Fujishima and K. Honda: Electrochemical photolysis of water at a semiconductor electrode. *Nature*, **238**, 5358 p.37-38 (1972).
- 3) T. Nonami and H. Taoda: Apatite Formation on TiO_2 Photocatalyst Film in a Pseudo Body Solution. *Materials Research Bulletin*, **33**, 1, p.125-132 (1998).
- 4) T. Suzuki and Y. Hayakawa: Proc. First Int Congr. on Phosphorus Compounds IMPHOS Paris, p.381 (1977).

- 5) T. Suzuki, T. Hatsushika, and Y. Hayakawa: Synthetic hydroxyapatites employed as inorganic cation exchangers. *J. Chem. Soc. Faraday Trans.*, **77**, 5, p.1059-1062 (1981).
- 6) T. Suzuki, T. Hatsushika, and M. Miyake: Synthetic hydroxyapatites as inorganic cation exchangers. Part 2. *J. Chem. Soc. Faraday Trans. I*, **78**, 12, p.3605-3611 (1982).
- 7) M. Miyake, T. Kobayashi, and T. Suzuki: Structural change of synthetic hydroxyapatite by ion-exchange reaction; cation-exchange characteristics for tin(2+) ions. *Yogyo-Kyokai-Shi*. (in Japanese), **94**, 8, p.832-836 (1986).
- 8) M. Miyake, K. Ishigaki, and T. Suzuki: Structure refinements of Pb²⁺ ion-exchanged apatites by x-ray powder pattern-fitting. *J. Solid State Chem.*, **61**, 2, p.230-235 (1986).
- 9) Y. Tanizawa, T. Ujiie, K. Sawamura, and T. Suzuki: Reaction characteristics between dental apatite and tin(2+) ion. (in Japanese), *Denki Kagaku oyobi Kogyo Butsuri Kagaku*, **55**, 12, p.903-908 (1987).
- 10) Y. Tanizawa, K. Sawamura, and T. Suzuki: Reaction characteristics of dental and synthetic apatites with iron(II) and iron(III) ions. *J. Chem. Soc. Faraday Trans.*, **86**, 7, p.1071-1075 (1990).
- 11) Y. Tanizawa, K. Sawamura, and T. Suzuki: Reaction characteristics of dental and synthetic apatites with aluminum(III) and lanthanum(III) ions in acidic solutions. *J. Chem. Soc. Faraday Trans.*, **86**, 24, p.4025-4029 (1990).
- 12) T. Suzuki and T. Hatsushika: Lattice-ion reaction characteristics of hydroxyapatite for iron(2+), iron(3+), and lead(2+) ions in acidic aqueous solutions. (in Japanese), *Gypsum and Lime*, **224**, p.15-20 (1990).
- 13) C. C. Ribeiro, M. A. Barbosa, and A. A. S. C. Machado: Modifications in the molecular structure of hydroxyapatite induced by titanium ions. *J. Material Science Material in Medicine*, **6**, 12, p.829-834 (1995).
- 14) S. R. Leadley, M. C. Davies, C. C. Ribeiro, M. A. Barbosa, A. J. Paul, and J. F. Watts: Investigation of the dissolution of the bioceramic hydroxyapatite in the presence of titanium ions using ToF-SIMS and XPS. *Biomaterials*, **18**, 4, p.311-316 (1997).
- 15) E. Wieser, I. Tsyganov, W. Matz, H. Reuther, S. Oswald, T. Pham, and E. Richter: Modification of titanium by ion implantation of calcium and/or phosphorus. *Surface and Coatings Technology*, **111**, 1, p.103-109 (1999).
- 16) H. Zeng, K. K. Chittur, and W. R. Lacey: Analysis of bovine serum albumin adsorption on calcium phosphate and titanium surfaces. *Biomaterials*, **20**, 4, p.377-384 (1999).
- 17) K. Kandori, T. Shimizu, A. Yasukawa, and T. Ishikawa: Adsorption of bovine serum albumin onto synthetic calcium hydroxyapatite: influence of particle texture. *Colloids and Surfaces B*, **5**, 1/2, p.81 (1995).
- 18) K. Kandori, N. Horigami, H. Kobayashi, A. Yasukawa, and T. Ishikawa: *J. Colloid Interface Sci.*, **191**, p.498 (1997).
- 19) Q. L. Feng, T. N. Kim, J. Wu, E. S. Park, J. O. Kim, D. Y. Lim, and F. Z. Cui: Antibacterial effects of Ag-HAp thin films on alumina substrates. *Thin Solid Films*, **335**, 1-2, p.214-219 (1998).
- 20) M. Wakamura, K. Kandori, and T. Ishikawa: Surface composition of calcium hydroxyapatite modified with metal ions. *Colloids and Surfaces A*, **142**, 1, p.107-116 (1998).
- 21) M. Wakamura, K. Kandori, and T. Ishikawa: Surface structure and composition of calcium hydroxyapatites substituted with Al(III), La(III) and Fe(III) ions. *Colloids and Surfaces A*, **164**, 23, p.297-305 (2000).
- 22) M. Wakamura, K. Kandori, and T. Ishikawa: Influence of chromium(III) on the formation of calcium hydroxyapatite. *Polyhedron*, **16**, 12, p.2047-2054 (1997).
- 23) Y. Kikuchi, K. Sunada, T. Iyoda, K. Hashimoto, and A. Fujishima: Photocatalytic bactericidal effect of TiO₂ thin films: dynamic view of the active oxygen species responsible for the effect. *Journal of Photochemistry and Photobiology A*, **106**, 1-3, p.51-56 (1997).
- 24) T. Ishikawa, M. Wakamura, and S. Kondo: Surface characterization of calcium hydroxyapatite by Fourier transform infrared spectroscopy. *Langmuir*, **5**, 1, p.140-144 (1989).



Masato Wakamura received the M.S. degree from Osaka University of Education, Osaka, Japan in 1987. He joined Fujitsu Ltd., Osaka, Japan in 1987 and then moved to Fujitsu Laboratories Ltd., Atsugi, Japan in 1989, where he has been engaged in research and development of inorganic functional materials. He has been a researcher of the Research Center for Advanced Science and Technology (RCAST) in Tokyo University since 1998 and is also a member of the Chemical Society of Japan.

E-mail: wakamura.masato@jp.fujitsu.com